Journal of Power Sources 240 (2013) 351–358

Contents lists available at SciVerse ScienceDirect

Journal of Power Sources

journal homepage: www.elsevier.com/locate/jpowsour

Fabrication of function-graded proton exchange membranes by electron beam irradiation for polymer electrolyte fuel cells under nonhumidified condition

Ryota Tsuchida [a,*], Atsushi Tsukamoto [a], Satoshi Hiraiwa [a], Akihiro Oshima [b], Masakazu Washio [a]

[a] Research Institute for Science and Engineering, Waseda University, 3-4-1, Okubo, Shinjuku, Tokyo 169-8555, Japan
[b] Institute of Scientific and Industrial Research, Osaka University, 8-1, Mihogaoka, Ibaraki, Osaka 567-0047, Japan

HIGHLIGHTS

- Function-graded PEMs (G-PEMs) for PEFC are fabricated by EB grafting method.
- G-PEMs have water uptake gradient in the thickness direction.
- XPS indicated that G-PEMs have different amount of SO_3^- between surface and back.
- G-PEMs have higher performance than Nafion®212 at 30 °C.
- G-PEMs have less temperature dependency than Nafion®212.

ARTICLE INFO

Article history:
Received 20 December 2012
Received in revised form
14 March 2013
Accepted 25 March 2013
Available online 2 April 2013

Keywords:
Polymer electrolyte fuel cell
Fuel cells
Electron beam
Proton exchange membranes
Radiation-grafting
Function-graded PEMs

ABSTRACT

Function-graded proton exchange membranes (G-PEMs) for polymer electrolyte fuel cells (PEFCs) are fabricated by electron beam (EB) grafting using a heterogeneous energy deposition technique. The fabricated G-PEMs have a water uptake gradient in the direction of the thickness originating from the sulfonic acid group gradient. Normal PEMs (N-PEMs), which have almost no gradient ionic groups in the membrane, are also fabricated to compare with G-PEMs. PEFC operations for comparing the fabricated G-PEMs, normal PEMs (N-PEMs), and Nafion®212 are carried out at 30 °C and 60 °C with dry H_2/O_2 gases. It is expected that the advantages of using dry fuel gases are lower cost and a smaller size system than that is possible with a humid fuel. The fabricated G-PEMs show a higher power density than Nafion®212 and N-PEMs at 30 °C, and the deterioration of the performance of fabricated G-PEMs is lower than that of Nafion®212. These results are thought to be caused by the difference in proton transfer kinetics between the fabricated G-PEMs and those of Nafion®212. It is therefore considered that G-PEMs not only exhibit higher performance at low temperature under nonhumidified conditions but also cost less than Nafion®212.

1. Introduction

Fuel cells (FCs), a power source employing H_2 and O_2, have attracted much attention as alternative energy resources. They emit no CO_2, SO_x, or NO_x, and may therefore be a possible solution to environmental problems. Regarding polymer electrolyte fuel cells (PEFCs) in particular, many attempts have been made to apply these types of fuel cells as power sources for mobile systems, houses, cars, submarines, and planes [1–3]. However, PEFCs have some problems that prevent their wide-spread use, such as fabricating cost, system size, and stability.

FCs are being introduced steadily, but decreasing the cost is needed for further growth. Proton exchange membranes (PEMs) such as Nafion® (DuPont) are key materials in PEFCs. Nafion® is known as a good and popular PEM, but its cost is high [4]. Thus, the development of low-cost PEMs is highly desirable.

The radiation-induced grafting of styrene and its derivatives into fluorinated polymer membranes and successive sulfonation was designed to be an alternative way to synthesize low-cost PEMs for PEFCs [5–24]. Our research group has studied partially fluorinated sulfonic acid membranes (part-FSAs) by the electron beam (EB) grafting method [8,14–17,20–22,25–27]. Furthermore, some researchers have reported that part-FSAs could demonstrate long term PEFC operations more than 10,000 h without significant increase of resistance [19,28].

* Corresponding author. #103, R.J. Shillman Hall, 3-14-9, Okubo, Shinjuku, Tokyo 169-0072, Japan. Tel./fax: +81 3 5286 2917.
E-mail address: ry_tsuchi@toki.waseda.jp (R. Tsuchida).

0378-7753/$ – see front matter © 2013 Elsevier B.V. All rights reserved.
http://dx.doi.org/10.1016/j.jpowsour.2013.03.120

In our previous study on the synthesis of function-graded partially fluorinated sulfonic acid membranes (G-PEMs) for PEFCs using low-energy EB irradiation [29,30], performance of FCs could be improved by controlling water uptake gradation in the membrane electrode assembly (MEA) through proton transportation direction. Sulfonic acid groups in G-PEMs have a graded density in the thickness direction, so that in this case, the gradient hydrophilic sulfonic acid group (SO_3^-) induces water uptake gradation. G-PEMs might therefore lead to significantly improved FCs in terms of higher performance and the ability to maintain stable operation.

Regarding FC size, downsizing is one of the most important issues for further growth in the use of FCs [31,32]. The downsizing of FC systems can be realized by improving the performance per unit size and the simplification of various components, especially the humidification devices, cooling equipment, and so on. If a humidification device is not assembled, PEFCs show lower performance under nonhumidified conditions than they do under humidified conditions because PEMs accomplish proton transfer through the hydrophilic sulfonic acid group SO_3^- under humidified conditions. On the other hand, when the FCs are operated at low temperatures, heaters and heat-insulating materials are not required. Hence, in this study, PEMs that show high performance under nonhumidified conditions at low temperature were fabricated and evaluated.

2. Method

2.1. Fabrication of G-PEMs

Poly(tetrafluoroethylene-co-hexafluoropropylene) (FEP, Flon Industry, Japan) films, each with a thickness of 50 μm, were used for the experiments. Depth-dose EB profiles were simulated by Monte Carlo simulation code EGS5. The FEP films were irradiated by EB with a low-energy EB accelerator (installed at RISE, Waseda University, CURETRON® NHV Corp.) under nitrogen atmosphere at room temperature (RT: 25 °C). To fabricate G-PEMs, a stack of two FEP layers was irradiated three times at 160 kV, and the second layer (50–100 μm) was selected for the grafting experiments because of the strong heterogeneous energy deposition, as shown in Fig. 1 (beam current: 1 mA). To evaluate the performance of G-PEMS by comparison, N-PEMs, which have almost no gradient ionic groups in the membrane, were obtained by one time EB irradiation of the first layer (0–50 μm) at 200 kV with homogeneous energy deposition (beam current: 1 mA). Each irradiated FEP film was grafted with liquid-phase styrene at 80 °C for 24 h. The degree of grafting (DOG) was calculated by the change in the weight.

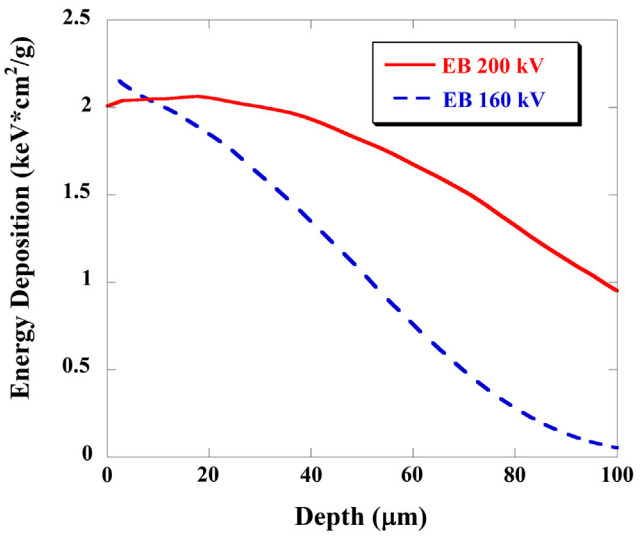

Fig. 1. Soft-EB depth–dose profiles in FEP calculated by EGS5.

The grafted samples were then sulfonated with chlorosulfonic acid in carbon tetrachloride (1:100, v/v) at RT for 24 h. Subsequently, they were soaked in deionized water at RT and treated in 1 M HCl for 24 h to obtain acidic-form PEMs. The obtained G-PEMs would have a water uptake gradient in the thickness direction because the irradiated films have an electron beam energy deposition gradient.

2.2. Evaluation of performance

The water uptakes of the obtained PEMs were measured at RT. Ion exchange capacities (IECs) were determined by an acid–base titration method using the 716 DMS Titrino automatic titrator (Metrohm-Herisaus). The obtained PEMs were evaluated in terms of the difference in chemical structure between the EB incident side (front-face) and the EB transmitted side (back-face) by XPS JPS-9010 (JEOL). The obtained G-PEMs were evaluated in terms of sulfonic acid group distribution in the thickness direction with SEM (S-3000-N, Hitachi) with an energy dispersive X-ray spectroscopy (EDX, EDAX) analysis.

Each PEM was laminated with Pt/C electrodes (Electro Chem, EC-E20-10-07, Pt loading at 1.0 mg cm^{-2}) to form the MEAs. The electrode which was standardized the amount of Pt loading at the anode and the cathode was purchased. The electrodes were coated with 25 μL cm^{-2} of Nafion® dispersion (DuPont, DE-521) and subsequently dried at 80 °C for 2 h to form binding layers on the electrodes. Each MEA was obtained by a press machine (Tester Sangyo, Japan) at 110 °C for 3 min with the pressure of 8.0 MPa. These MEAs were assembled into a standard single cell with an effective area of 1.0 cm^2.

Each PEM was evaluated in terms of FC performance at 30 °C and 60 °C using dry H_2 and dry O_2 under pressures of 0.2 MPa and a flow rate of 50 mL min^{-1}. The evaluation was made in terms of polarization performance and electrochemical impedance spectroscopy (EIS) with a HZ-3000 electrochemical analysis system (Hokuto Denko). EIS was measured in the frequency range from 100 kHz to 0.1 Hz at the ac current density of 500 mA cm^{-2}.

3. Results and discussion

3.1. Fabrication of G-PEMs

Fig. 1 shows the depth–dose profiles for the low-energy EB simulated by EGS5 code. The simulation model of the low-energy EB is composed of three layers: the top layer is titanium foil [thickness: 12.7 μm, charge density (ρ): 4.50 g cm^{-3}], the middle layer is nitrogen atmosphere (thickness: 7.0 cm, ρ: 1.25×10^{-3} g cm^{-3}), and the bottom layer is the FEP sample (thickness: 100 μm, ρ: 2.15 g cm^{-3}). A total of 1.0×10^7 electrons were irradiated for the simulation and the results were averaged to obtain the data. The energy deposition depends on the accelerating voltages in the FEP films. Energy deposition gradually decreases with increasing distance from the surface (EB incident side). In the case of lower acceleration voltages, the results indicate that heterogeneous energy deposition is taking place in the medium. Moreover, the energy deposition changes significantly around the EB terminal region. This means that function-controlled materials could be synthesized by selection of an appropriate accelerating voltage and irradiation region. Thus, G-PEMs could be fabricated by irradiation at 160 kV in the region 50–100 μm using a heterogeneous energy deposition technique. On the other hand, for EBs accelerated by high voltage, the energy deposition occurs almost homogeneously in the shallow region, as shown in Fig. 1. It is thought that N-PEMs, which have

homogeneous sulfonic acid group distribution, could be fabricated by the irradiation at 200 kV in the region 0–50 μm.

According to the EGS5 simulation, the total energy deposition at 160 kV irradiation is lesser than that at 200 kV. Therefore, to obtain an equal amount of free radicals induced by the irradiations at both 200 kV and 160 kV, the FEP layers in the region 0–50 μm are irradiated once at 200 kV and the layers in the region 50–100 μm are irradiated three times at 160 kV. Although the simulated total energy deposition of 200 kV irradiation in FEP is smaller than that of three times irradiation at 160 kV, the trapped radicals at 200 kV irradiation show almost equivalent to three times one at 160 kV because of their annihilation. As a result, FEP was irradiated three times at 160 kV.

3.2. Characteristic properties of PEMs

The DOG, wet thickness, water uptake, and ion exchange capacity (IEC) of the obtained PEMs are summarized in Table 1. Although the average doses between N-PEM and G-PEM are equal, the average DOG for N-PEM is higher than that of G-PEM. Because energy deposition is minimal at around the EB stopping range, either the quantity of sufficient radicals for the grafting reaction might not have been induced in G-PEM or the actual parameters in the experiments might have shifted to the smaller values as compared to the simulation model. Moreover, in the case of G-PEM, because the radical yields have a gradient in the thickness direction, the permeation of the styrene monomer from the film surface to the inside of the film might occur heterogeneously. Another reason may have been that the annihilation of radicals took place in the EB incident surface due to the high-energy deposition. Thus, the DOG of G-PEM would appear lower than that of N-PEM.

Although the values for the water uptake and wet thickness of N-PEM and G-PEM are almost identical, the IEC of N-PEM is higher than that of G-PEM, and it is found that the IEC results correspond to those of the DOG.

The average water uptakes of our fabricated PEMs are about 2.5 times higher than those of Nafion®212. The average IECs of N-PEM and G-PEM are 1.9 and 1.5 times higher, respectively, than that of Nafion®212. Probably, the difference arises between G-PEM and N-PEM because of the comparison of average ones. The results indicate that the water uptake depends on the density and the distribution of the sulfonic acid groups.

Fig. 2 shows the S_{2p} XPS spectra of both N-PEM and G-PEM. The strong peak at around 168 eV, which is assigned to the sulfonic acid group SO_3^-, is detected in both PEMs. For the peak intensities of G-PEM, a large difference between the EB incident side (denoted as "front-face") and the EB transmitted side (denoted as "back-face") is observed, in which the intensity of the front-face is 13 times higher than that of back-face. Thus, G-PEM has a different amount of sulfonic acid groups between the front-face and back-face. Moreover, to analyze the more detail information in inner region of G-PEMs, the plasma etching was carried out for thickness direction and then was measured by XPS. That is, front-face (0 μm), back-face (69 μm from front-face at dry condition) and plasma etched samples (25 μm, 44 μm from the front-face) were measured. The S_{2p} peak intensity was gradually decreased from front-face to back-face. It is suggested that G-PEM has the sulfonic acid group

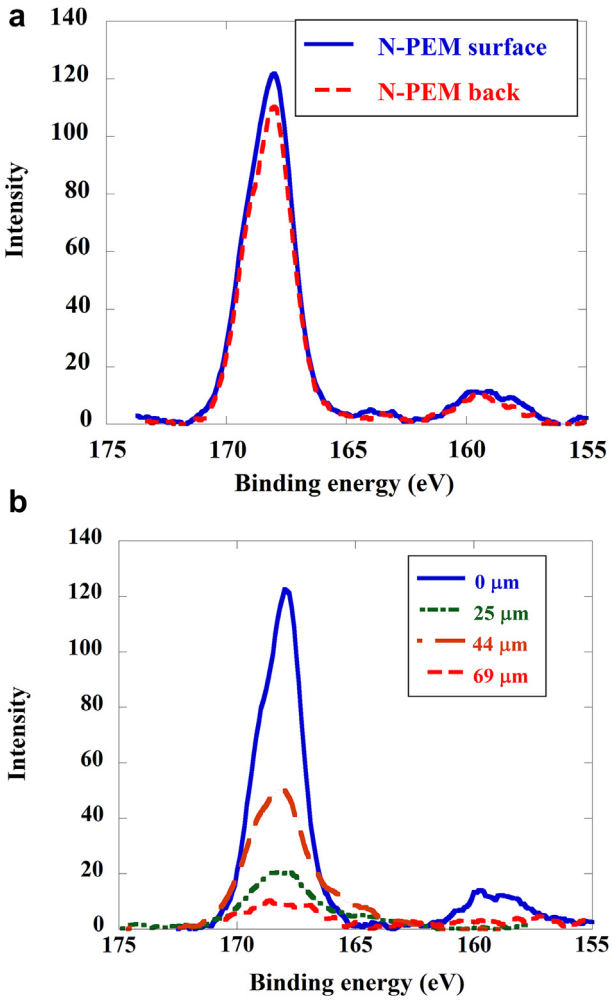

Fig. 2. XPS spectra of (a) N-PEM and (b) G-PEMs (0 μm from front-face, 25 μm from front-face, 44 μm from front-face and 69 μm from front-face).

gradient in the direction of the thickness owing to the heterogeneous energy deposition technique. On the other hand, in the case of N-PEM, the peak intensities of both surfaces (front-face and back-face) are almost identical. It is found that the homogeneous grafting reaction would be induced with our experimental setup of EB irradiation as simulated by ESG5.

Fig. 3 shows the SEM image and SEM-EDX analysis of cross-section for typical G-PEM with polyvinyl chloride boards. The left side is back-face of G-PEM and the right side is front-face. The sulfur element distribution which corresponds to sulfonic acid group distribution in G-PEM was graded from front-face to back-face.

On the other hand, in our previous study, N-PEM has shown the homogeneous distribution of sulfonic acid groups in the direction of thickness [30]. Therefore, it is suggested that the G-PEMs which would have sulfonic acid group gradient could be fabricated with EB grafting using a heterogeneous energy deposition technique.

3.3. Fuel cell performance

As described above, the synthesized G-PEM has a sulfonic acid group gradient in the direction of the thickness. MEAs based on G-PEMs (G-MEAs) can be classified into two types: decreased ionic sites from the anode to the cathode side in the FC (denoted as "decrease-type") and increased ionic sites from the anode to the cathode (denoted as "increase-type"). Fig. 4 shows decrease-type

Table 1
Characteristic properties of PEMs.

	DOG (%)	Water uptake (%)	Wet thickness (μm)	IEC (meq g^{-1})
N-PEM	40.8	64	92	1.89
G-PEM	32.8	60	88	1.51
Nafion®212	–	25	62	0.97

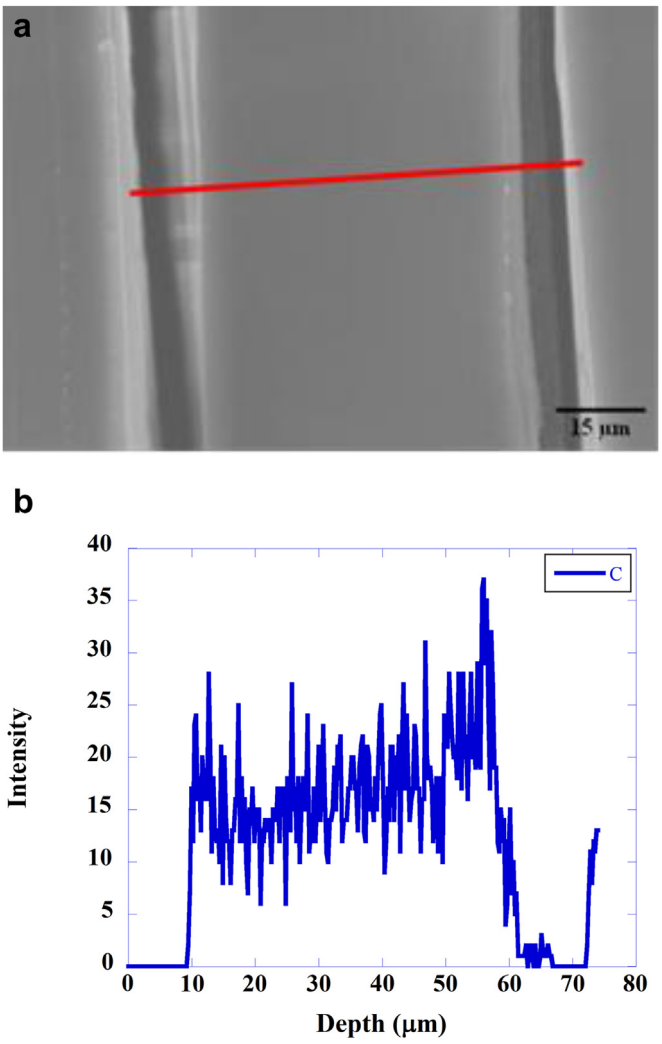

Fig. 3. SEM-EDX analysis of typical G-PEM in direction of thickness (a) SEM image and (b) sulfur distribution spectra.

G-MEA and increase-type G-MEA model. Decrease-type G-MEAs consist of a rich sulfonic acid group on the anode side and a poor sulfonic acid group on the cathode side. However, increase-type G-MEAs consist of a rich ionic site on the cathode side and a poor ionic site on the anode side. This means that the rich and poor ionic sites show hydrophilic and hydrophobic properties, respectively.

The FC performance is evaluated at 30 °C and 60 °C with dry H_2/O_2 gases. Fig. 5 shows FC performance at 30 °C and 60 °C under non-humidified conditions for N-MEA based on N-PEM, increase- and decrease-type G-MEAs, and Nafion®212. The FC performance of each MEA is listed in Table 2. The performances at 30 °C are lower than those at 60 °C for all PEMs because catalytic activity and kinetic energy decrease with decreasing temperature [33].

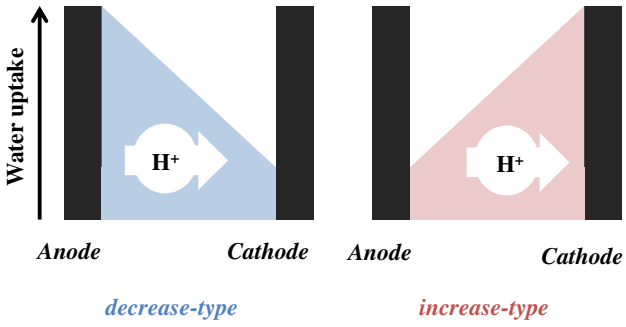

Fig. 4. Concepts of decrease- and increase-type of G-PEMs.

For the FC operations at 30 °C and 60 °C, the power densities at both 500 mA cm^{-2} and maximum of both increase- and decrease-type G-MEAs are higher than those of N-MEAs. The power densities at 60 °C of both types of G-MEAs are similar to those of Nafion® 212. However, the power densities of both types of G-MEAs at 30 °C are higher than those of Nafion®212. Thus, it is found that the decrease in FC performance from 60 °C to 30 °C using G-MEAs is lower than that using Nafion®212. That is, G-PEMs and N-PEMs fabricated by the EB-grafting method are less temperature-dependent than Nafion®212. Especially at 30 °C, decrease-type G-MEAs show the least temperature dependency, with a maximum power density of 421 mW cm^{-2} and the highest performance of all tested MEAs.

It is considered that the reason for the difference in temperature dependency between our fabricated part-FSAs and Nafion®212 could be explained by the differences in proton transfer. In general, two types of proton transfer models are known: one is the Vehicle mechanism and the other one is the Grotthuss (hopping) mechanism. The Vehicle mechanism means that the oxonium ion (H_3O^+) in a water molecule (H_2O) cluster, which is formed by protons bound to H_2O, would be transported in PEMs from anode to cathode. With the Grotthuss mechanism, protons are directly conducted (through hopping) on H_2O molecules trapped in a sulfonic acid group. Proton transfer by the Vehicle mechanism should be more temperature-dependent than that by the Grotthuss mechanism because of the mobility of the H_2O cluster [34–36].

Our part-FSA fabricated by EB-grafting is considered to be strongly influenced by direct proton transport on H_2O molecules trapped within sulfonic acid groups [37]. As a result, the proton conductivity of our fabricated PEM is only minimally influenced by the mobility of H_2O clusters even at lower temperatures, and thus, the conduction of protons via the Grotthuss mechanism plays an important role. Thus, G-MEAs would show higher performance than Nafion®212 at 30 °C.

Furthermore, decrease-type G-MEAs show higher performance than increase-type G-MEAs in the higher current density regions. It is considered that proton conductivity due to the Vehicle mechanism might be assisted by the water uptake gradient of decrease-type G-MEAs. Decrease-type G-MEAs are function-graded in the thickness direction, and they have more sulfonic acid groups and higher water uptake on the anode side than on the cathode one. It is suggested that the rich water uptake at the anode side could be efficiently maintained as the proton produced with a Pt catalyst can be made to conduct directly.

In general, FC performance in higher current density regions was decreased by dry-up in nonhumidified condition. For our fabricated G-MEAs, it is considered that the water uptake graduation would be prevented from drying-up. Especially, for decrease-type G-MEAs, the water uptake gradient from cathode (poor amount of water) to anode (rich one) would easily induce the back diffusion.

Although the major proton transport model of our fabricated part-FSA membrane is the Grotthuss mechanism [37], in the case of decrease-type G-MEAs, it is considered that the produced protons would happen from the anode to the cathode not only by direct hopping (i.e., the Grotthuss mechanism) but also indirectly through transportation via oxonium ion (H_3O^+) because of the high water uptake on the anode side. It is thought that transporting of H_3O^+ is stimulated by the water uptake gradient from the anode to cathode side.

Fig. 6 shows the Cole–Cole plots from EIS. The ohmic resistance (R_{ohm}) and charge transfer resistance (R_{ct}) are calculated by the fitting from the Cole–Cole plots, as listed in Table 3. Here, R_{ohm} is

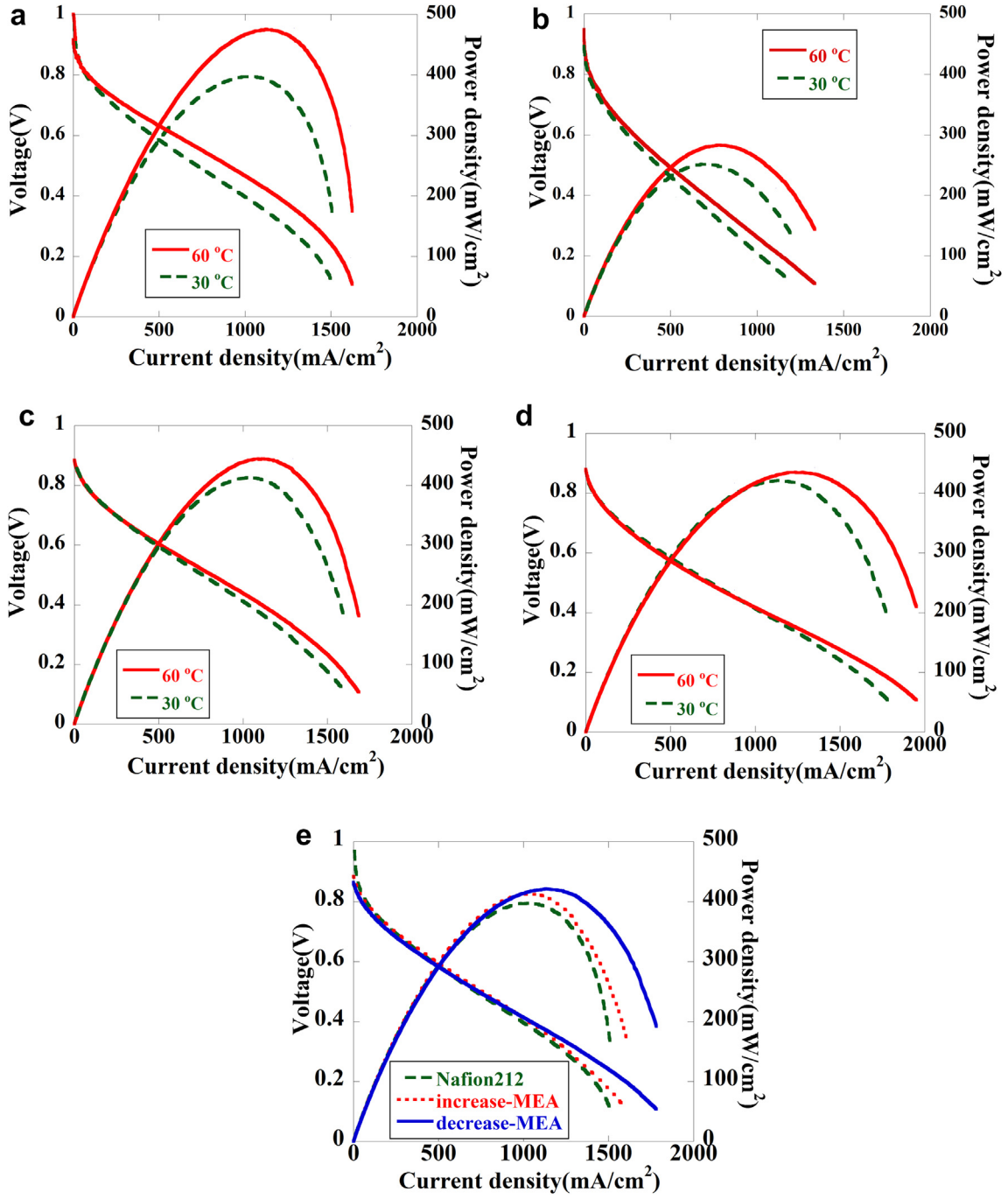

Fig. 5. Polarization curves of (a) Nafion®212, (b) N-MEA, (c) increase-type G-MEA, (d) decrease-type G-MEA, and (e) at 30 °C under nonhumidifying conditions.

the intersection on the real axis at high frequency, whereas R_{ct} is the diameter of the semicircle on the real axis. R_{ct} is contributed by activation polarization and diffusion polarization. Comparing EIS values between 30 °C and 60 °C under nonhumidified conditions, it is found that R_{ct} for both fabricated PEMs and Nafion®212 increases with decreasing temperature.

On the other hand, although R_{ohm} for Nafion®212 increases with decreasing temperature, R_{ohm} for our fabricated PEMs show equivalent values, regardless of temperature. R_{ohm} is the membrane resistance, which is one of the indexes of proton conductivity in an electrolyte. Hence, it is suggested that our fabricated PEMs using EB-grafting method would be strongly influenced by the Grotthuss mechanism.

Regarding lower frequency regions, Nafion® had additional resistance, which would indicate the dry-up in nonhumidified condition [38,39]. On the contrary, for our fabricated MEAs based on part-FSAs (N-PEM and G-PEM) show the lower resistance compared with Nafion®. Thus, the fabricated MEAs would be prevented from drying-up because of their different proton conducting mechanism, higher IEC and back water diffusion. In the near future, more detail analysis of water distribution in G-PEM should be carried out with neutron beam scattering experiments during FC operation.

Table 3 also shows the calculated ionic conductivity (IC) and activation energy. As the R_{ohm} and the IC for our fabricated N-PEM and G-PEM showed almost equivalent values, regardless of

Table 2
Cell performance of each membrane.

Sample	Temperature (°C)	Wet thickness (μm)	Power density (mW cm^{-2})	
			At 500 mA cm^{-2}	Maximum
Nafion®212	60	62	315	475
	30		292	397
N-PEM	60	92	246	283
	30		230	252
Increase-type of G-MEA	60	88	302	445
	30		298	413
Decrease-type of G-MEA	60	88	287	435
	30		292	421

Table 3
Electrochemical impedance analysis data of each MEA.

Sample	Temperature (°C)	R_{ohm} (ohm cm^2)	R_{ct} (ohm cm^2)	IC (mS cm^{-1})	Activation energy (kJ mol^{-1})
Nafion®212	60	0.09	0.28	69	10.3
	30	0.13	0.30	48	
N-MEA	60	0.10	0.60	92	–
	30	0.10	0.62	92	
Increase-type of G-MEA	60	0.11	0.34	80	–
	30	0.11	0.39	80	
Decrease-type of G-MEA	60	0.11	0.31	80	–
	30	0.11	0.34	80	

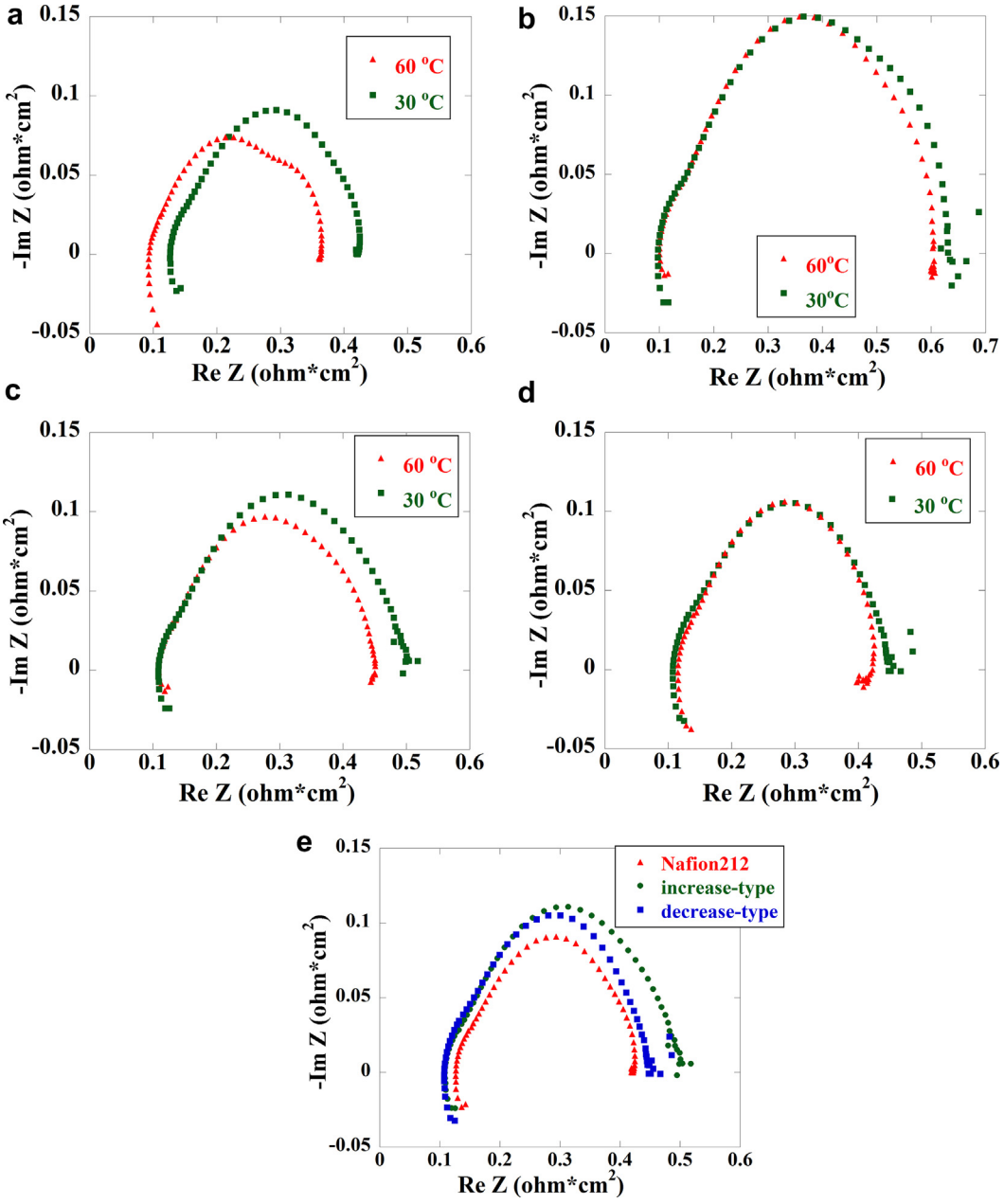

Fig. 6. Electrochemical impedance spectra of (a) Nafion®212, (b) N-MEA, (c) increase-type G-MEA, (d) decrease-type G-MEA, and (e) at 30 °C under nonhumidifying conditions.

different temperatures, the activation energy couldn't be estimated by Arrhenius plots. In the case of Nafion® 212, the activation energy was 10.3 kJ mol^{-1}, as same as previous reports [40,41].

In our previous work, the activation energy of part-FSA which was estimated from Arrhenius plots of ionic conductivities, showed lower than that of Nafion®212 [27]. In the case of Grotthuss mechanism, it is well known that the activation energy is lower than that of Vehicle mechanism [34,41]. That is, it is suggested that proton transporting mechanism of our fabricated PEMs would be strongly influenced by the Grotthuss mechanism, comparison with Vehicle mechanism [41–43].

In general, it is well known that the thinner PEMs show higher IC [44,45]. Although our fabricated G-PEM is about 1.5 times thicker than Nafion®212, the FC performance of G-PEM at 30 °C under the nonhumidified conditions is higher than that of Nafion®212. Therefore, it is considered that G-PEMs operating at low temperature under nonhumidified conditions would be superior to Nafion®212 in terms of FC performance. It is expected that our fabricated G-PEMs, which can utilize the dry fuel gases, are lower cost and smaller than normal PEMs using a humid fuel-supplying system.

4. Conclusion

Function-graded PEMs (G-PEMs) were fabricated by EB grafting using a heterogeneous energy deposition technique. G-PEMs have a sulfonic acid group gradient in the direction of the thickness. Comparison of the FC performance at 30 °C and 60 °C showed that the deterioration of FC performance of our fabricated PEMs was lower than that of Nafion®212. Hence, the temperature dependencies of the fabricated PEMs in terms of FC performance were smaller than that of Nafion®212. The results could be explained by the difference in proton transfer kinetics between our fabricated PEMs and Nafion®212. Furthermore, the decrement of the FC performance in the higher current regions using G-PEM was lower than that of Nafion212®. It is suggested that the fabricated G-MEAs would be prevented from drying-up because of their different proton conducting mechanism, higher IEC and back diffusion. It is considered that G-PEMs would have not only better performance at low temperature under nonhumidified condition but also less cost than Nafion®212.

Acknowledgments

A part of this work was supported by RISE project of Waseda University (11L01). A part of this work was supported by Low Carbon Network Project (Handai satellite) of Ministry of Education, Culture, Sports, Science and Technology (MEXT), Japan.

References

[1] H. Inaka, S. Sumi, K. Nishizaki, T. Tabata, A. Kataoka, H. Shinkai, Journal of Power Sources 106 (2002) 60–67.
[2] F.N. Buchi, G. Paganelli, P. Dietrich, D. Laurent, A. Tsukada, P. Varenne, A. Delfino, R. Kotz, S.A. Freunberger, P.A. Magne, D. Walser, D. Olsommer, Fuel Cells 7 (2007) 329–335.
[3] M.T. Gencoglu, Z. Ural, International Journal of Hydrogen Energy 34 (2009) 5242–5248.
[4] J. Marcinkoski, J.P. Kopasz, T.G. Benjamin, International Journal of Hydrogen Energy 33 (2008) 3894–3902.
[5] F.N. Buchi, B. Gupta, O. Haas, G.G. Schere, Electrochimica Acta 40 (1995) 345–353.
[6] F.N. Buchi, B. Gupta, O. Haas, G.G. Scherer, Journal of The Electrochemical Society 142 (1995) 3044–3048.
[7] M.M. Nasef, H. Saidi, H.M. Nor, O.M. Foo, Journal of Applied Polymer Science 78 (2000) 2443–2453.
[8] K. Sato, S. Ikeda, M. Iida, A. Oshima, Y. Tabata, M. Washio, Nuclear Instruments & Methods in Physics Research, Section B 208 (2003) 424–428.
[9] T.R. Dargaville, G.A. George, D.J.T. Hilla, A.K. Whittaker, Progress in Polymer Science 28 (2003) 1355–1376.
[10] T. Yamaki, M. Asano, Y. Maekawa, Y. Morita, T. Suwa, J. Chen, N. Tsubokawa, K. Kobayashi, H. Kubota, M. Yoshida, Radiation Physics and Chemistry 67 (2003) 403–407.
[11] M.M. Nasef, E.A. Hegazy, Progress in Polymer Science 29 (2004) 499–561.
[12] T. Yamaki, K. Kobayashi, M. Asano, H. Kubota, M. Yoshida, Polymer 45 (2004) 6569–6573.
[13] L. Gubler, H. Kuhn, T.J. Schmidt, G.G. Scherer, H.P. Brack, K. Simbeck, Fuel Cells 4 (2004) 196–207.
[14] J.Y. Li, K. Sato, S. Ichiduri, S. Asano, S. Ikeda, M. Iida, A. Oshima, Y. Tabata, M. Washio, European Polymer Journal 40 (2004) 775–783.
[15] J.Y. Li, K. Sato, S. Ichiduri, S. Asano, S. Ikeda, M. Iida, A. Oshima, Y. Tabata, M. Washio, European Polymer Journal 41 (2005) 547–555.
[16] J.Y. Li, S. Ichizuri, S. Asano, F. Mutou, S. Ikeda, M. Iida, T. Miura, A. Oshima, Y. Tabata, M. Washio, Applied Surface Science 245 (2005) 260–272.
[17] J.Y. Li, S. Ichizuri, S. Asano, F. Mutou, S. Ikeda, M. Iida, T. Miura, A. Oshima, Y. Tabata, M. Washio, Nuclear Instruments & Methods in Physics Research, Section B 236 (2005) 333–337.
[18] L. Gubler, N. Prost, S.A. Gursel, G.G. Scherer, Solid State Ionics 176 (2005) 2849–2860.
[19] L. Gubler, S.A. Gursel, G.G. Scherer, Fuel Cells 5 (2005) 317–335.
[20] S. Asano, F. Mutou, S. Ichizuri, J.Y. Li, T. Miura, A. Oshima, Y. Katsumura, M. Washio, Nuclear Instruments & Methods in Physics Research, Section B 236 (2005) 437–442.
[21] A. Oshima, T. Miura, S. Asano, S. Ichizuri, J.Y. Li, S. Ikeda, M. Iida, C. Matsuura, Y. Tabata, Y. Katsumura, M. Washio, Research on Chemical Intermediates 31 (2005) 585–593.
[22] J.Y. Li, A. Matsuura, T. Kakigi, T. Miura, A. Oshima, M. Washio, Journal of Power Sources 161 (2006) 99–105.
[23] T. Yamaki, J. Tsukada, M. Asano, R. Katakai, M. Yoshida, Journal of Fuel Cell Science and Technology 4 (2007) 56–64.
[24] M. Zhai, S. Hasegawa, J. Chen, Y. Maekawa, Journal of Fluorine Chemistry 129 (2008) 114–119.
[25] A. Matsuura, T. Kakigi, Y. Sato, K. Fujii, N. Mitani, J.Y. Li, A. Oshima, M. Washio, Macromolecular Symposia 249–250 (2007) 221–227.
[26] Y. Sato, K. Fujii, N. Mitani, A. Matsuura, T. Kakigi, F. Mutou, J.Y. Li, A. Oshima, M. Washio, Nuclear Instruments & Methods in Physics Research, Section B 265 (2007) 213–216.
[27] F. Muto, A. Oshima, T. Kakigi, N. Mitani, A. Matsuura, K. Fujii, Y. Sato, J.Y. Li, M. Washio, Nuclear Instruments & Methods in Physics Research, Section B 265 (2007) 162–167.
[28] J. Huslage, H.P. Brack, F. Geiger, F.N. Buchi, A. Tsukada, G.G. Scherer, PSI Scientific Report 1998, Annex V (1999), pp. 51–52.
[29] H. Fujita, F. Shiraki, T. Yoshikawa, A. Oshima, M. Washio, Journal of Photopolymer Science and Technology 23 (2010) 387–392.
[30] H. Fujita, F. Shiraki, Y. Oshima, T. Tatsumi, T. Yoshikawa, T. Sasaki, A. Oshima, M. Washio, Radiation Physics and Chemistry 80 (2011) 201–206.
[31] H. Yoshida, T. Hyakudome, S. Ishibashi, T. Sawa, S. Tsukioka, T. Aoki, T. Tani, M. Iwata, T. Moriga, ECS Transactions 26 (2010) 67–76.
[32] K. Kikuchi, I. Kato, M. Yoshida, M. Wada, S. Mizuno, ECS Transactions 16 (2008) 1901–1906.
[33] I. Gatto, A. Stassi, E. Passalacqua, A.S. Arico, International Journal of Hydrogen Energy 30 (2012) 1–7.
[34] K.D. Kreuer, A. Rabenau, W. Weppner, Angewandte Chemie, International Edition 21 (1982) 208–209.
[35] K.D. Kreuer, Chemistry of Materials 8 (1996) 610–641.
[36] G.A. Luduea, T.D. Kuhne, D. Sebastiani, Chemistry of Materials 23 (2011) 1424–1429.
[37] A. Oshima, Y. Sato, F. Shiraki, N. Mitani, K. Fujii, Y. Oshima, H. Fujita, M. Washio, Radiation Physics and Chemistry 80 (2011) 164–168.
[38] M. Gomadam, W. Weidner, International Journal of Energy Research 29 (2005) 1133–1151.
[39] C. Isami, K. Sufiura, A. Daigo, T. Murakami, The Electrochemical Society 42 (2012) 171–178.
[40] J. Malm, F.N. Buchi, O. Haas, M. Stamm, G.G. Scherer, Electrochimica Acta 39 (8/9) (1994) 1303–1307.
[41] M. Saito, K. Hayamizu, T. Okada, Journal of Physics and Chemistry B 109 (2005) 3112–3119.
[42] Y. Sone, P. Ekdunge, D. Simonsson, Journal of Electrochemical Society 143 (4) (1996) 1254–1259.
[43] A.Z. Weber, J. Newman, Journal of The Electrochemical Society 151 (2) (2004) A311–A325.
[44] A. Bayrakceken, S. Erkan, L. Turker, I. Eroglu, International Journal of Hydrogen Energy 33 (2008) 165–170.
[45] S. Hiraiwa, T. Yoshikawa, A. Oshima, M. Washio, Journal of Photopolymer Science and Technology 25 (2012) 481–485.

Glossary

G-PEMs: function-graded proton exchange membranes
PEFCs: polymer electrolyte fuel cells
EB: electron beam
XPS: X-ray photoelectron spectroscopy

FC: fuel cell
part-FSA: partially fluorinated sulfonic acid membrane
MEA: membrane electrode assembly
SO_3^-*:* sulfonic acid group
FEP: poly(tetrafluoroethylene-co-hexafluoropropylene)
RT: room temperature: 25 °C
N-PEMs: normal PEMs
N-MEA: MEA based on N-PEMs
DOG: degree of grafting
IC: ionic conductivity
IEC: ion exchange capacities
front-face: EB incident side
back-face: EB transmitted side
EIS: electrochemical impedance spectroscopy
G-MEA: MEA based on G-PEM
decrease-type: decreased ionic sites from anode to cathode in FC cell
increase-type: increased ionic sites from anode to cathode in FC cell
H_3O^+*:* oxonium ion
R_{ohm}*:* ohmic resistance
R_{ct}*:* charge transfer resistance